THE JOURNAL OF PHYSICAL CHEMISTRY B

Article

pubs.acs.org/JPCB

Selection of Ionic Liquids for Enhancing the Gas Solubility of Volatile Organic Compounds

Maria Gonzalez-Miquel,[†] Jose Palomar,*[,‡] and Francisco Rodriguez[†]

[†]Departamento de Ingeniería Química, Universidad Complutense de Madrid, 28040 Madrid, Spain

[‡]Sección de Ingeniería Química (Departamento de Química Física Aplicada), Universidad Autónoma de Madrid, Cantoblanco, 28049 Madrid, Spain

Supporting Information

ABSTRACT: A systematic thermodynamic analysis has been carried out for selecting cations and anions to enhance the absorption of volatile organic compounds (VOCs) at low concentration in gaseous streams by ionic liquids (ILs), using COSMO-RS methodology. The predictability of computational procedure was validated by comparing experimental and COSMO-RS calculated Henry's law constant data over a sample of 125 gaseous solute−IL systems. For more than 2400 solute−IL mixtures evaluated, including 9 solutes and 270 ILs, it was found that the lower the activity coefficient at infinite dilution (γ^{∞}) of solutes in the ILs, the more the exothermic excess enthalpy (H^{E}) of the equimolar IL−solute mixtures. Then, the solubility of a representative sample of VOC solutes, with very different chemical nature, was screened in a wide number of ILs using COSMO-RS methodology by means of γ^{∞} and H^{E} parameters, establishing criteria to select the IL structures that promote favorable solute−solvent intermolecular interactions. As a result of this analysis, an attempt of classification of VOCs respect to their potential solubility in ILs was proposed, providing insights to rationally select the cationic and anionic species for a possible development of absorption treatments of VOC pollutants based on IL systems.

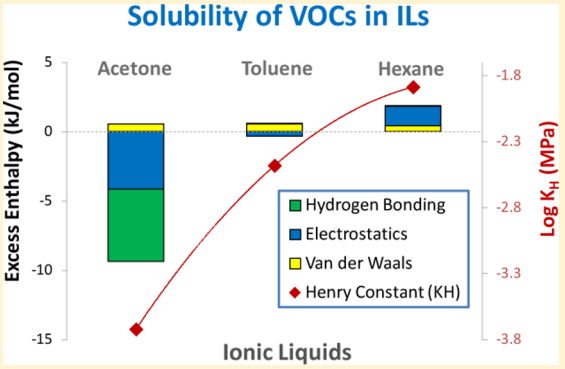

1. INTRODUCTION

Room-temperature ionic liquids (ILs) are a broad category of organic salts which have being receiving growing attention in both academia and industry during the past decade.[1−3] The unique properties of these novel solvents, such as their low vapor pressures and tailorability (i.e., the possibility of selecting/designing the adequate cations and anions to obtain a solvent with specific properties), have made them attractive for a wide variety of engineering applications.[4−7] In particular, the use of ILs as media in gas separation processes appears specially promising, to the effect that they are being broadly investigated as absorbents for a variety of gaseous compounds including CO_2,[8−16] H_2S,[17] H_2,[14,15,18−21] inert gases,[19,20,22,23] N_2,[10,11,19,20] O_2,[8,11,20] SO_2,[8,24] NH_3,[25,26] and VOCs such as alkanes,[8−12,19,20,23,27,28] alkenes,[8,9,11,12,27,28] hydrofluorocarbons,[29−31] dimethyl sulfide, dimethyl disulfide and toluene.[32,33]

Considering the huge variety of cation and anion combinations for possible ILs, computational methods to estimate thermodynamic properties have been demonstrated of great utility for preselecting the best cation−anion combinations for a specific IL application. At this point, COSMO-RS (Conductor-like Screening Model for Real Solvents) developed by Klamt and co-workers is regarded as a valuable method to predict the thermodynamic properties of ILs mixtures on the basis of unimolecular quantum chemical calculations for the individual molecules,[34,35] providing an a priori computational tool for designing ILs with the required properties.[36,37] In fact, several publications have shown the general suitability of COSMO-RS method to predict properties of IL systems, including the solubilities and Henry's law constants of several gases in ILs.[25,26,33,38−43] Moreover, an important feature is that the different intermolecular interactions (electrostatic forces, hydrogen bonding and van der Waals forces) between the mixture components can be quantified by COSMO-RS, contributing to the interpretation of gas solubility in ILs from a molecular point of view.[44] In our previous works, COSMO-RS was successfully used as a guide for driving a rational selection of ILs with upgraded features for several gas absorption applications.[25,26,33,40,41] An appreciable input for understanding the physical absorption of CO_2 and the CO_2/N_2 selectivity in ILs was reported on the basis of an energetic analysis performed for the excess enthalpies and the intermolecular interactions of the solute−IL mixtures, with results leading to propose novel brominated-based ILs with optimized characteristics for CO_2 capture[40] and [SCN^-]-based ILs to be applied as solvents in supported ionic liquid membranes (SILMS) for CO_2/N_2 separation processes.[41] In addition, an innovative computational−experimental research

Received: October 23, 2012
Revised: December 13, 2012

   dx.doi.org/10.1021/jp310499p | J. Phys. Chem. B XXXX, XXX, XXX−XXX

strategy was developed to propose optimized ILs for gas absorption, including novel task-specific ILs such as [EtOHmim][BF_4] and [choline][NTf_2] for ammonia absorption,[25,26] and commercially available imidazolium-[NTf_2] ILs for toluene absorption,[33] with experimental evidences supporting the favorable thermodynamic and kinetic performance of the selected solvents.

Volatile organic compounds (VOCs) are well-known as common air pollutants characterized by their high vapor pressures and low boiling points.[45] Recovery of VOCs from industrial atmospheric emissions has become a great challenge in the last decades, prompted by specific international legislations[46,47] which limit the concentration for VOCs emissions into atmosphere. In this regard, the development of novel absorption techniques based on ILs is being considered as a potential alternative to efficiently recover VOCs, overcoming the disadvantages (i.e., high volatily, toxicity and flammability) of the organic solvents used in conventional absorption processes.

Under this scenario, the aim of this paper is to serve as a guide for selecting cations and anions to form IL structures with optimized properties to enhance the gas solubility of VOCs at low concentrations. For this purpose, a systematic theoretical analysis of the solute−ILs thermodynamics and energetic interactions was carried out by applying COSMO-RS methodology, which involved the following steps:

(i) Evaluating the capability of COSMO-RS to predict the solubility behavior of different solutes in ILs: the experimental versus the computed values of the Henry's law constants of more than 125 solute−IL systems were compared.

(ii) Analyzing the relationship between the activity coefficient at infinite dilution (γ^{∞}) of solutes in ILs and the excess enthalpy (H^E) of the equimolar IL−solute mixtures: the activity coefficients (γ^{∞}) of more than 2400 solute−IL mixtures, including 9 solutes (acetone, benzene, chloroform, ethane, ethene, phenol, H_2S, H_2 and trifluoroethane) and 270 ILs (considering 15 anions of diverse nature and 18 cations from different families, see Table 1) were computed by COSMO-RS and related with the excess enthalpy (H^E) of the liquid mixtures, in order to compare the affinity of ILs for solutes with very different vapor pressure.

(iii) Classification of the gaseous compounds attending to both the volatility of the solutes and their activity coefficients in ILs: from the analysis of the computed and reported experimental data, different cases regarding gaseous compounds were detected, ranging from aliphatic compounds, which showed high positive deviations from Raoult's law (low solubility in ILs) to polar organic solutes, which presented remarkably negative deviations from ideality (high solubility in ILs).

(iv) Systematic gas solubility and energetic COSMO-RS analysis of the solute−IL systems focused on three common indoor VOC solutes,[48] i.e. acetone, phenol, and chloroform: first, the chemical nature of the gases and the IL solvents was analyzed by means of the polarized charge distributions on the molecular surfaces provided by COSMO-RS. Then, COSMO-RS screenings of the Henry's law constants of the selected solutes in 270 representative ILs were carried out to obtain an overall picture of the gas solubility behavior of the systems. Afterward, the contributions of the intermolecular interactions (misfit-electrostatic, hydrogen bonding, and van der Waals) to the excess enthalpy of the IL−solute mixture were analyzed to determine their effects on the physical solubility of these VOCs in the ILs.

(v) Providing a general evaluation of the influence of the IL structure on the solubility of a representative sample of VOCs: the COSMO-RS screening was extended to analyze the activity coefficients and intermolecular interactions of 14 VOC solutes with different chemical nature in ILs, selecting those cations and anions that provided, respectively, the highest negative and positive deviations from the ideality and, consequently, the potentially most favorable and unfavorable properties to absorb VOCs.

Table 1. List of Ionic Liquids

abbreviation	name
	Cations
eim^+	1-ethylimidazolium
$emim^+$	1-ethyl-3-methylimidazolium
$emmim^+$	1-ethyl-2,3-dimethylimidazolium
OH-$emim^+$	1-(2-hydroxyethyl)-3-methylimidazolium
meO-$emim^+$	1-(2-methoxypropyl)-3-methylimidazolium
ph-$emim^+$	1-(phenylethyl)-3-methylimidazolium
$bmim^+$	1-butyl-3-methylimidazolium
$hxmim^+$	1-hexyl-3-methylimidazolium
$omim^+$	1-octyl-3-methylimidazolium
$dcmim^+$	1-decyl-3- methylimidazolium
bpy^+	1-butylpyridinium
$1b3mpy^+$	1-butyl-1-methylpyridinium
$bmpyr^+$	1-butyl-1-methylpyrrolidinium
$bpyr^+$	1-butylpyrrolidinium
$1b4DMApy^+$	1-butyl-4-(dimethylamino)pyridinium
b-M^+	1-butylmorpholinium
b-Q^+	1-butylquinolinium
bbbb-P^+	tetrabutylphosphonium
bbbb-N^+	tetrabutylammonium
$choline^+$	(2-hydroxyethyl)trimethylammonium
	Anions
BF_4^-	tetrafluoroborate
$FeCl_4^-$	tetrachloroferrate
$CF_3CO_2^-$	trifluoroacetate
$CF_3SO_3^-$	trifluorosulfonate
$CH_3CO_2^-$	acetate
SCN^-	methanesulfonate
$C_4H_{10}PO_4^-$	diethylphosphate
$formate^-$	formate
DCN^-	dicyanamide
FEP^-	tris(pentafluoroethyl)trifluorophosphate
NO_3^-	nitrate
$BC_4N_4^-$	tetracyanoborate
PF_6^-	hexafluorophosphate
$C(CN)_3^-$	methanetricarbonitrile
NTf_2^-	bis(trifluoromethylsulfonyl)imide

2. COMPUTATIONAL METHODOLOGY

The molecular geometry of all compounds (solutes and ILs counterions) was optimized at the B3LYP/6-31++G** computational level in the ideal gas phase using the quantum chemical Gaussian 03 package.[49] A molecular model of independent counterions was applied in COSMO-RS calculation, where ILs are treated as equimolar mixture of cation and anion.[40] Vibrational frequency calculations were performed in each case to confirm the presence of an energy minimum. Once molecular models were optimized, Gaussian03 was used to

dx.doi.org/10.1021/jp310499p | J. Phys. Chem. B XXXX, XXX, XXX−XXX

compute the COSMO files. The ideal screening charges on the molecular surface for each species were calculated by the continuum solvation COSMO model using BVP86/TZVP/DGA1 level of theory. Subsequently, COSMO files were used as an input in COSMOthermX[50] code to calculate the thermodynamic properties (Henry's law constants and activity coefficients of solutes in ILs, and detailed excess enthalpies contributions of solute−IL mixtures) and to compute the σ-profiles of the compounds. According to our chosen quantum method, the functional and the basis set, we used the corresponding parametrization (BP_TZVP_ C21_0111) that is required for the calculation of physicochemical data and that contains intrinsic parameters of COSMOtherm, as well as specific parameters.

Alternatively, Henry's law constants can be determined from the COSMO-RS calculations using the semiempirical Antoine equation to estimate the vapor pressure in the expression:

$$K_H = \gamma_i^{\infty} p_0^{vap} \quad (1)$$

where K_H is the Henry's law constant, γ_i^{∞} is the activity coefficient of the solute at infinite dilution in the IL calculated by COSMOthermX, and p_0^{vap} is the vapor pressure of the pure gas, estimated by either COSMOthermX or the Antoine equation (obtained from NIST database).

3. RESULTS

3.1. Gas Solubilities in ILs from COSMO-RS Analysis.

The capability of COSMO-RS to predict the solubility behavior of different solutes in ILs was evaluated by comparing the experimentally available Henry constants ($K_{H,experimental}$) to the computed Henry constants ($K_{H,COSMO-RS}$) of more than 125 solute−IL systems,[8−33] including 27 solutes and 24 ILs, with a wide variety of cations and anions. The comparisons include compounds of very different nature such as inert gases, aromatics, alkanes, and alkenes, or gases like CO_2, SO_2, or H_2S, which present a wide range of Henry constant values (i.e., from 0.005 MPa for toluene in [dcmim][NTf_2] to 602.6 MPa for H_2 in [bmim][CH_3SO_4]) at near room temperature and atmospheric pressure. Based on results of Figure 1, it is concluded that a priori COSMO-RS method provides reasonably predictions of the solubility behaviors of gas solutes in ILs for the whole range of K_H values reported in the literature, as indicated by the goodness-of-fit between the experimental and the computed data in Figure 1A (slope = 1.09, square correlation coefficient R^2 = 0.88, and standard deviation σ = 0.88). Note that the vapor pressures used to perform the Henry constant calculations in Figure 1A were those estimated by COSMO-RS methodology. Meanwhile, Figure 1B shows the comparison between the experimental and the computed K_H values of the systems when implementing the empirical Antoine equation to calculate the vapor pressure of the solutes. The statistical parameters (slope = 0.93, R^2 = 0.89, and σ = 0.85) show a slightly enhanced agreement between the predicted and the experimental values of the Henry constants of the solutes in the ILs. In general, implementing empirical equations to determine the vapor pressure of the solutes instead of using the vapor pressure estimated by COSMO-RS methodology in Version C2.1 Release 01.11 of COSMO*therm* does not lead to significant changes in the overall data predictions. However, it might be appropriate to consider the empirical vapor pressure of specific solutes such as CO_2 or H_2S, whose values are not well estimated by the used version of

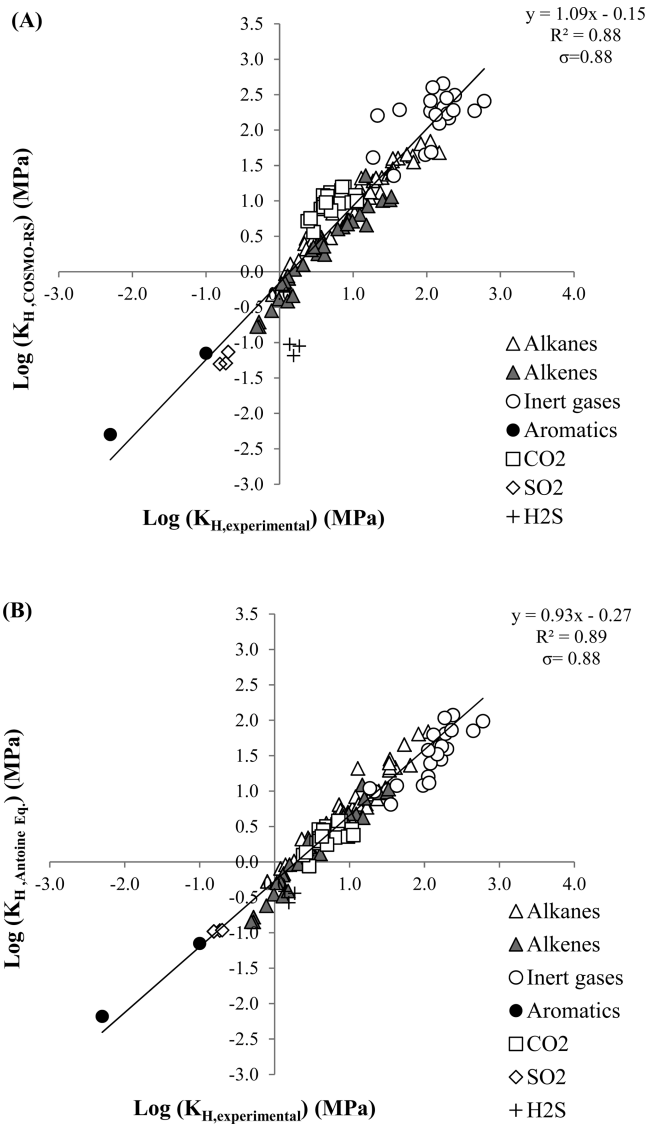

Figure 1. Experimental vs COSMO-RS Henry constants of solutes in ILs at near-ambient temperature and atmospheric pressure using vapor pressures of pure compounds (A) predicted by COSMO-RS and (B) estimated by empirical Antoine equation.

COSMO-RS method, hence providing some discrepancies between the experimental and the estimated solubility behavior of the solutes. For instance, an overestimation of the CO_2 vapor pressure ($P_{vap,COSMO-RS}$ = 29 794.3 kPa versus $P_{vap,empirical}$ = 7186.5 KPa) leads to estimated Henry constant values 2-fold higher than the experimentals (i.e., $K_{H,COSMO-RS}$ = 15.9 MPa versus $K_{H,exptl}$ = 7.6 MPa for CO_2 in [bmim][BF_4]); on the contrary, the underestimation of the H_2S vapor pressure ($P_{vap,COSMO-RS}$ = 501.14 kPa versus $P_{vap,empirical}$ = 7186.5 KPa) leads to lowering the estimated Henry constant values (i.e., $K_{H,COSMO-RS}$ = 1.55 MPa versus $K_{H,exptl}$ = 0.07 MPa for H_2S in [bmim][BF_4]).

Previous studies by our group evidenced relationships between the Henry constants of the gas solutes in the ILs and the excess enthalpy (H^E) of the IL−solute liquid mixture for the cases of CO_2, N_2, NH_3, and toluene compounds,[25,26,33,40,41] with results illustrating that the higher the exothermicity of the mixture (or the stronger intermolecular interactions between the solute and the solvent), the higher the

dx.doi.org/10.1021/jp310499p | J. Phys. Chem. B XXXX, XXX, XXX−XXX

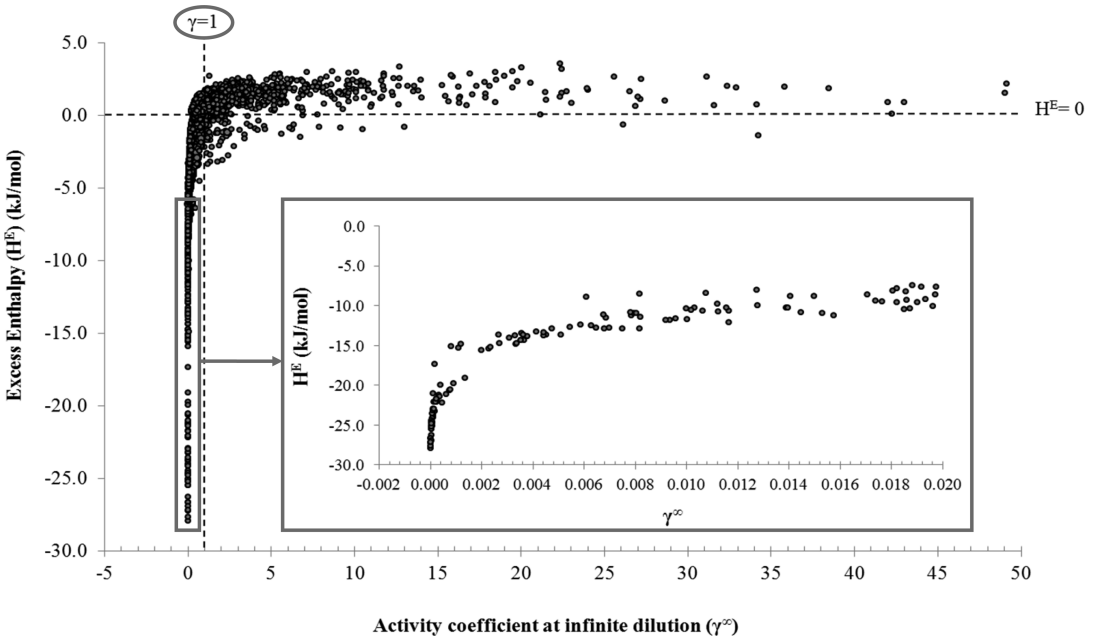

Figure 2. Relationship between the excess enthalpies (H^E) of IL−solute equimolar mixtures and the activity coefficients at infinite dilution (γ^∞) of solutes in ILs (T = 298 K, P = 1 bar).

Table 2. Classification of Gaseous Solutes in Terms of Their Solubilities in ILs

	phase at 298 K and 1 atm			
	condensed		gaseous	
favorable interactions [AM(γ^∞) < 1]	1	acetone, phenol, chloroform	2	alkanes (C < 2), alkenes (C < 2) fluoroalkanes, fluoroalkenes (C < 2) CO_2, SO_2, NH_3, H_2S, H_2
unfavorable interactions [AM(γ^∞) > 1]	3	toluene, benzene	4	alkanes (4 > C > 2), alkenes (4 > C > 2) Ar, N_2, Xe, O_2

solubility of the solute in the IL (this is the lower Henry constant values). In this work, the activity coefficient at infinite dilution (γ^∞) of more than 2400 solute−IL mixtures, including 9 solutes (acetone, benzene, chloroform, ethane, ethane, phenol, H_2S, H_2, and trifluoroethane) and 270 ILs, were related to the excess enthalpy of the IL−solute mixtures, both computed by COSMO-RS (Figure 2). Considering the activity coefficients instead of the Henry constants allows leaving aside the effect of the very different vapor pressure of the 9 pure solute compounds studied. The screening included ILs based on different cation families (imidazolium, pyridinium, pyrrolidinium, phosphonium, ammonium, quinolinium, and morpholinium) and a wide variety of anions ([FEP$^-$], [NTf_2^-], [$FeCl_4^-$], [$CF_3SO_3^-$], [$CF_3CO_2^-$], [$B(CN)_4^-$], [NO_3^-], [$CH_3CO_2^-$],[$CH_3PO_4^-$], [$C(CN)_3^-$], [DCN$^-$], [BF_4^-], [SCN$^-$], [PF_6^-], and [CHOO$^-$], see Table 1). In Figure 2, two different areas can be distinguished based on the activity coefficient values: the one corresponding to negative deviation from Raoult's law (γ^∞ < 1) and the other corresponding to positive deviation from Raoult's law (γ^∞ > 1). It can be seen that the solutes−IL systems presenting activity coefficients γ^∞ < 1 are related to an exothermic behavior of the liquid mixture, where the attractive forces between molecules of solute and IL are greater than the solute−solute or IL−IL cohesive forces. In these cases, the partial vapor pressure of the solute component in the mixture is lower than that expected from Raoult's law, implying an enhanced solubility of the gas solute in the IL solvent because of their mutual chemical affinity. In fact, it can be appreciated in the enlarged area of Figure 2 that the higher the exothermicity of the liquid mixture, the lower the activity coefficient of the solute in the solvent, related to the more favorable intermolecular interactions between IL and solute respect to the pure compounds. These results suggest that the systems showing negative deviations from Raoult's law involve solutes which can be better absorbed by ILs. On the contrary, those solute−IL systems setting along the area corresponding to γ^∞ > 1 present an excess enthalpy of the mixture around zero value, which implies no particular affinity between the molecules of the solute and the IL solvent; these systems present a partial vapor pressure of the solute higher than that of the pure compound and, consequently, a lower absorption capacity of the solutes in the ILs.

The trends explained above suggest the possibility of classifying the different solubility behaviors of the gases in the ILs attending to the volatility of the solutes and their activity coefficients in ILs. An attempt at classifying the solutes included in Figure 1 (whose gas solubility behavior has been experimentally measured in bibliography) is presented in Table 2, attending to both the γ^∞ values of each one of the solutes in ILs (either those reported in bibliography or those calculated by COSMO-RS in 270 ILs) and the phase state of the compounds at 298 K and 1 atm. These criteria lead to differentiate four groups of solutes. (i) Group 1, those with low volatility (which are in condensed phase at 298 K and 1 atm) showing attractive interactions with ILs [i.e., AM (γ^∞) < 1, where AM stands for the arithmetic mean]. The solutes of this group correspond to VOCs functionalized with strong polar compounds, as acetone, chloroform, and phenol. They present

dx.doi.org/10.1021/jp310499p | J. Phys. Chem. B XXXX, XXX, XXX−XXX

Table 3. VOCs−ILs Systems Exhibiting (A) Minimum and (B) Maximum Values of Activity Coefficients at Infinite Dilution (γ^{∞}) and Henry Constants (K_H) Provided by COSMO-RS Screening over 135 Imidazolium-Based ILs at 298 K[a]

(A) Potential Highest Gas Solubility					
VOC		best absorbent	γ^{∞} (min)	K_H (MPa)	main VOC−IL interactions[b]
favorable absorption	phenol	[emmim][acetate]	2.3×10^{-5}	4.3×10^{-9}	HB (f)
	acetone	[eim][FEP]	0.01	1.9×10^{-4}	HB (f) > MF (f)
	ethyl acetate	[eim][FEP]	0.02	1.4×10^{-4}	HB (f) > MF (f)
	chloroform	[emmim][acetate]	0.02	5.0×10^{-4}	HB (f) > MF (f)
	CH_2Cl_2	[emmim][acetate]	0.04	1.7×10^{-3}	MF (f) > HB (f)
moderate absorption	tetrafluoroethane	[omim][acetate]	0.27	1.6×10^{-1}	HB (f) > MF (f) > VDW (u)
	ethene	[omim][FEP]	0.48	2.9	VDW (u) ≫ MF (f)
	ethane	[omim][FEP]	0.73	6.0	MF (u) ≫ VDW (u)
	toluene	[omim][FEP]	0.77	3.3×10^{-3}	VDW (u) ≫ MF (f)
	benzene	[omim][FEP]	0.77	1.3×10^{-2}	VDW (u) ≫ MF (f)
unfavorable absorption	hexafluoroethane	[omim][FEP]	1.49	2.2	MF (u) ≫ VDW (u)
	CCl_4	[omim][FEP]	1.59	6.0	MF (u) > VDW (u)
	hexane	[omim][FEP]	1.83	1.0×10^{-1}	MF (u) ≫ VDW (u)
	octane	[omim][FEP]	2.69	1.3×10^{-2}	MF (u) ≫ VDW (u)
(B) Potential Lowest Gas Solubility					
VOC		worst absorbent	γ^{∞} (max)	K_H (MPa)	main VOC−IL interactions[b]
favorable absorption	phenol	[eim][FEP]	0.98	1.9 × 10−4	HB (u) > MF (f) ≈ VDW (u)
	acetone	[eim][Acetate]	2.05	3.7 × 10−2	HB (u) > MF (f)
	ethyl acetate	[eim][Acetate]	3.88	3.0 × 10−2	HB (u) > MF (f)
	chloroform	[eim][FEP]	1.29	2.8 × 10−2	VDW (u) ≫ MF (u)
	CH_2Cl_2	[eim][FEP]	0.72	3.4 × 10−2	VDW (u)
moderate absorption	tetrafluoroethane	[eim][FEP]	0.53	0.31	MF(u) > HB(u) ≈ VDW(u)
	ethene	[emim][DCN]	2.07	12.6	MF (u) > HB (u)
	ethane	[emim][DCN]	5.71	46.7	MF (u) > HB (u)
	toluene	[emim][DCN]	8.59	3.6 × 10−2	MF (u) > HB (u)
	benzene	[emim][DCN]	4.96	8.3 × 10−2	MF (u) > HB (u)
unfavorable absorption	hexafluoroethane	[emim][DCN]	263.04	395.0	MF (u) ≫ VDW (u)
	CCl_4	[emim][DCN]	34.31	0.4	MF (u) ≫ VDW (u)
	hexane	[emim][DCN]	109.29	6.1	MF (u) ≫ VDW (u)
	octane	[emim][DCN]	436.26	2.2	MF (u) ≫ VDW (u)

[a]Description of main VOC−IL intermolecular contributions obtained from the excess enthalpy of equimolar mixtures. [b]HB: Hydrogen bond; MF: polar-misfit; VDW: van der Waals. (f): favorable interactions; and (u): unfavorable interactions.

the lowest range of Henry constants in the ILs (always less than 0.1 MPa for all of the 270 ILs). (ii) Group 2: gaseous solutes at 298 K and 1 atm showing effective interactions with ILs [i.e., AM (γ^{∞}) < 1] such as short-chain alkanes and alkenes, or some gases like CO_2, SO_2, H_2, H_2S, and NH_3, which in general present Henry constants not higher than 50 MPa. (iii) Group 3: liquid solutes at 298 K and 1 atm showing unfavorable interactions with ILs [i.e., AM (γ^{∞}) > 1], such as the aromatic compounds benzene or toluene, which present Henry constants lower than 1 MPa. And (iv) Group 4: gaseous solutes which show unfavorable interactions with ILs [i.e., AM (γ^{∞}) > 1], such as inert gases (Ar, Xe, N_2) or other gaseous compounds such as O_2, which generally present Henry constants higher than 50 MPa. In summary, Table 2 exposes a wide range of gas solubility behaviors for VOCs in ILs, mainly depending on the chemical nature of the organic compounds and their structural features. In view of this, a deeper understanding of the IL−solute systems would be of great help for propounding effective industrial applications based on ILs to separate VOCs from gas streams. For this purpose, in this work the COSMO-RS computational analysis was first focused on three common indoor VOCs classified as group 1 in Table 2: acetone, phenol, and chloroform, which potentially present a favorable absorption in ILs. Later, the COSMO-RS analysis was extended to a representative sample of 14 organic compounds (see Table 3) from different nature in order to evaluate the overall trends of the solubility of VOCs in ILs.

3.2. Gas Solubility of Acetone in ILs. The COSMO-RS screening of the Henry constants of acetone in 270 ILs, including 18 cations based on different families and 15 different anions, is presented in Figure 3. The overall K_H values of acetone in the ILs are lower than 0.02 MPa, which indicates a general high gas solubility of this solute in ILs. Moreover, this screening shows that the solubility of acetone in ILs is mainly influenced by both the cation and the anion, with the value of the Henry constant of the solute differing by more than 1 order of magnitude depending on the ions of the solvents. Thus, cations that present functional groups with acidic character as hydroxyl (i.e., [OH-emim$^+$] or [choline$^+$]) and big anions with disperse charge (i.e., [FEP$^-$] or [NTf$_2^-$]) seem capable to provide much higher solubilities (lower Henry constants) of acetone in the IL solvent.

COSMO-RS method calculates the thermodynamic properties of fluid mixtures by using the polarized charge distribution of their individual compounds visualized as histogram σ-profiles.[14] Therefore, based on COSMO-RS methodology, the σ-profile of one compound includes the main chemical information necessary to predict its possible interaction in a fluid phase. The COSMO-RS histogram can be qualitatively divided into three main regions upon the following cutoff

dx.doi.org/10.1021/jp310499p | J. Phys. Chem. B XXXX, XXX, XXX−XXX

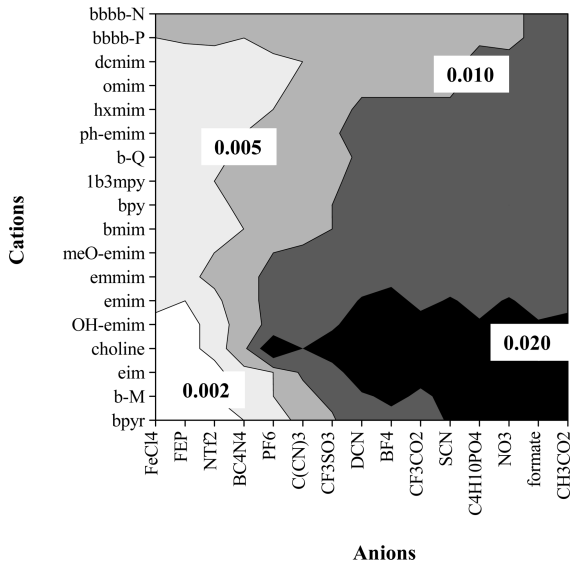

Figure 3. Screening of the Henry constants (MPa) of acetone in ILs at T = 298 K computed by COSMO-RS.

values: the hydrogen bond (HB) donor region (σ < −0.0082 e/Å^2), the HB acceptor region (σ > +0.0082 e/Å^2) and the nonpolar region (−0.0082 < σ < +0.0082 e/Å^2). An overview over the properties and usage of σ-profile can be found in refs 51 and 52. Figure 4A shows the σ-profile of the acetone solute, which presents a peak at +0.012 e/Å^2 resulting from the carbonyl oxygen that indicates HB acceptor capacity of the compound. On the contrary, the absence of a prominent peak in the region σ < −0.0082 e/Å^2 of the σ-profile of the acetone indicates that the solute does not show HB donor capacity. In addition, the broad distribution of charge on the σ polarity scale of Figure 4A represents the remarkably polar character of the acetone molecule. Therefore, from the analysis of the σ-profile of the acetone, it can be foreseen that ILs with HB donor groups (acidic character) might enhance its solubility. This premise leads to think about [eim$^+$] cation as an appropriate structure for enhancing the solubility of acetone because of the acidic character of N−H group, which is represented in the σ-profile of the cation in Figure 4B by a noticeable concentration of charge at the strong HB donor region (−0.21 e/Å^2). In fact, the acidic character of the imidazolium cations decreases with the increasing number of alkyl substituents attached to the imidazolium ring in the following order: [eim$^+$] > [emim$^+$] > [emmim$^+$], as clearly shown by their σ-profiles in Figure 4B. An alternative to confer acidic character to an imidazolium cation is its functionalization with hydroxyl group (see the case of [OH-emim$^+$] in Figure 4B). On other hand, anions are generally not able to establish hydrogen-bonding interactions with HB acceptor groups as acetone. However, Figure 4C shows that anions such as [$CH_3CO_2^-$] can present groups with located charge at positive σ region and, therein, basic character. Therefore, HB acceptor anions may promote anion−cation hydrogen bonding which would compete with acetone−cation interactions. On the contrary, big anions with disperse charge such as [FEP$^-$] are not strong HB acceptor species, which may allow enhancing the acetone solubility in the ILs based on this kind of anions. Once we analyzed the chemical nature of individual species in acetone−IL mixtures, the next step of COSMO-RS analysis was to relate the acetone solubility in ILs to the different intermolecular interactions contributing to the

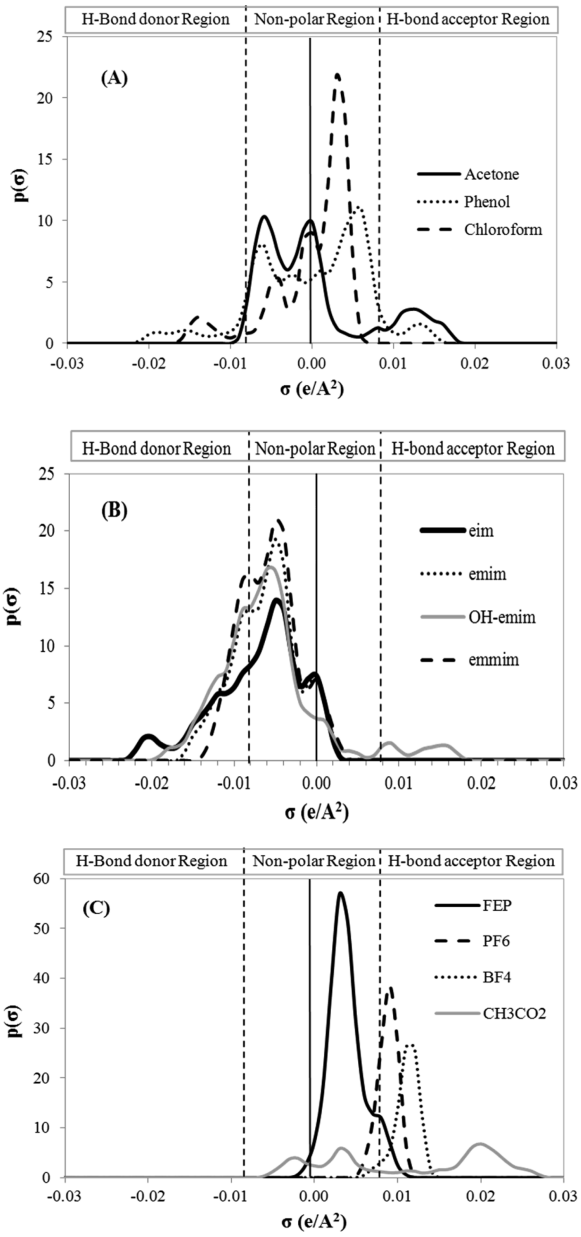

Figure 4. σ-Profiles of (A) VOC solutes, (B) IL cations, and (C) IL anions.

excess enthalpy of the acetone−IL equimolar mixtures. Figure 5 presents the relationship between K_H and H_E values for representative IL−acetone mixtures, showing the effect of the anion and the cation by the analysis, respectively, of IL common anion (Figure 5A) and cation (Figure 5B) series. Results indicated that the attractive hydrogen-bonding interactions (exothermic mixing process; i.e. negative values of H_E) between acetone and IL determine the increasing solubility of acetone in these solvents (decreasing K_H values). Meanwhile, the attractive electrostatic interactions (Misfit) between the polar solute and the polar solvents play a secondary role, and the van der Waals interactions make almost negligible contributions to the excess enthalpies of these systems. These results support that ions capable of increasing the solubility of acetone in ILs are those able to establish attractive hydrogen bonds in the mixture with acetone. Indeed, a further glance at the effect of the cation in Figure 5A

dx.doi.org/10.1021/jp310499p | J. Phys. Chem. B XXXX, XXX, XXX−XXX

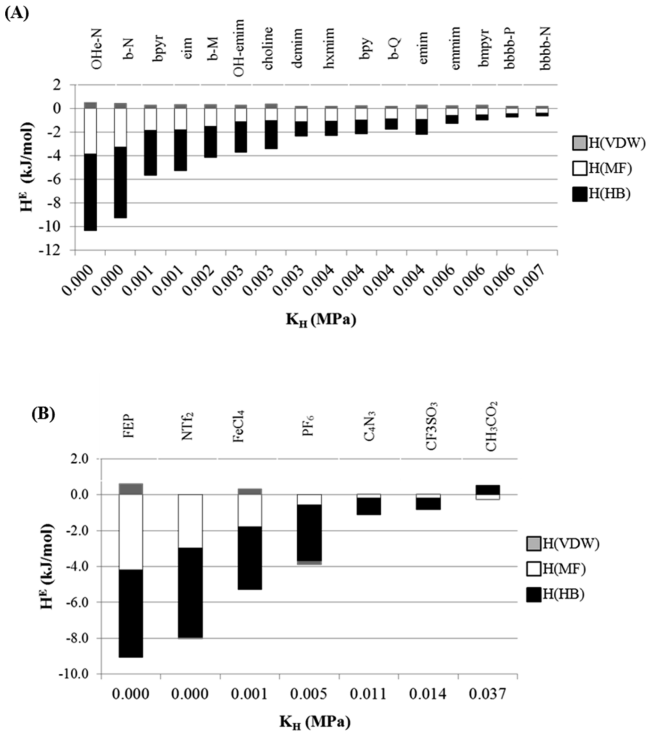

Figure 5. Relationship between the Henry constants (K_H) and the different intermolecular interaction contributions to the excess enthalpy [H(VDW), H(HB), and H(MF)] of acetone−IL systems at T = 298 K computed by COSMO-RS. (A) Effect of the cation considering NTf_2 as the common anion. (B) Effect of the anion considering eim as the common cation.

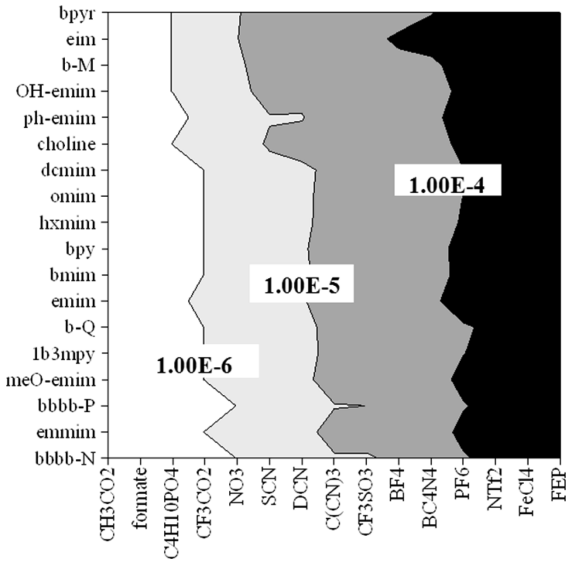

Figure 6. Screening of the Henry constants (MPa) of phenol in ILs at T = 298 K computed by COSMO-RS.

illustrates that for IL with common anion [NTf_2^-] the more the acidic groups in the cation ([eim^+] > [$emim^+$] > [$emim^+$] > [$emmim^+$]), the higher the solubility of this solute in ILs. In addition, those cations functionalized with acidic groups, such as OH^- or NH^-, significantly enhance the acetone solubility in ILs in relation to their nonfunctionalized analogues. It can be seen that cationic family does not have a significant impact on the solubility of the acetone in the ILs. On the other hand, if one considers a series of ILs with common cation ([eim^+] in Figure 5B) it is clear that big anions with disperse charge, such as [FEP^-] and [NTf_2^-], allow for better HB interaction between the solute and the cation, resulting in higher solubilities of acetone in ILs; this is the opposite of what happens with anions that present located charge and strong basic groups, such as [$CH_3CO_2^-$] or [$CF_3SO_3^-$], which tend to interact with the cation, hence hindering the effective interaction between the acetone and the ILs.

3.3. Gas Solubility of Phenol in ILs. Figure 6 shows the screening of the Henry constants of phenol in ILs computed by COSMO-RS. The extremely low K_H values of phenol in the ILs suggest the high capacity of this kind of solvents to absorb the phenol solute. As it is represented in Figure 6, the solubility of phenol in ILs is clearly controlled by the anions, whose adequate selection allows decreasing 2 orders of magnitude the K_H values. The solubility of phenol is enhanced by those anions presenting basic character, such as [$CH_3CO_2^-$], formate, or [$CF_3CO_2^-$] anions, and only slightly improved by cations without acidic hydrogen atoms like [bbbb-N^+] or [$emmim^+$]. This behavior can be attributed to the HB donor character of the solute molecule, as supported by the σ-profile of phenol in Figure 4A which presents a peak at −0.016 e/Å^2, assignable to the strong acidic hydrogen atom of the hydroxyl group of phenol. The relationship between the solubility of phenol in ILs (in terms of Henry constant) and the intermolecular interaction contributions to the excess enthalpy of the liquid mixture is depicted in Figure 7. This figure shows that exothermic HB contributions to the H_E of phenol−IL mixing process are related to decreasing Henry constants of this solute in the IL solvents. It indicates that the affinity between the acidic OH group of the solute and the HB acceptor groups of anions is controlling the solubility of the phenol in the ILs. This is the case of the acetate and formate anions, whose basic carboxyl groups are capable to effectively interact by HB formation with the hydroxyl group of the phenol. Note that the head family does not have a significant impact on the phenol solubility, although cations without acidic hydrogen atoms (like [bbbb-N^+] or [$emmim^+$]), and cation families with less HB donor character (i.e., imidazolium, ammonium, or posphonium rather than pyrrolidinim or morpholinium), slightly enhance the solubility of phenol in ILs. In sum, the selection of the anion is critical to boost the phenol absorption in ILs, since the anion plays the main role in establishing effective hydrogen-bonding interactions with this solute.

3.4. Gas Solubility of Chloroform in ILs. The COSMO-RS screening of the Henry constants of chloroform in ILs is presented in Figure 8. The K_H values of this solute in the sample of 270 ILs cover the range from 0.00 to 1.20 MPa (depending on the selection of the cation and anion), indicating the remarkable solubility of chloroform in the IL solvents. As for the case of the acetone, the solubility of chloroform in ILs is determined by both the cation and the anion. The σ-profile of chloroform (Figure 4A) shows three peaks in the nonpolar region corresponding to the carbon and chlorine atoms. However, the small peak located at the HB donor region (−0.014 e/Å^2) of the σ-profile, which is associated to the hydrogen atom, indicates a slightly acidic character and polarity of this solute. As shown in the screening (Figure 8), the solubility of chloroform is enhanced by ILs with the highest HB acceptor character, like those containing anions such as [$CH_3CO_2^-$], whereas a big anion with disperse charge as [FEP^-] or [NTf_2^-] does not promote favorable solute−IL

dx.doi.org/10.1021/jp310499p | J. Phys. Chem. B XXXX, XXX, XXX−XXX

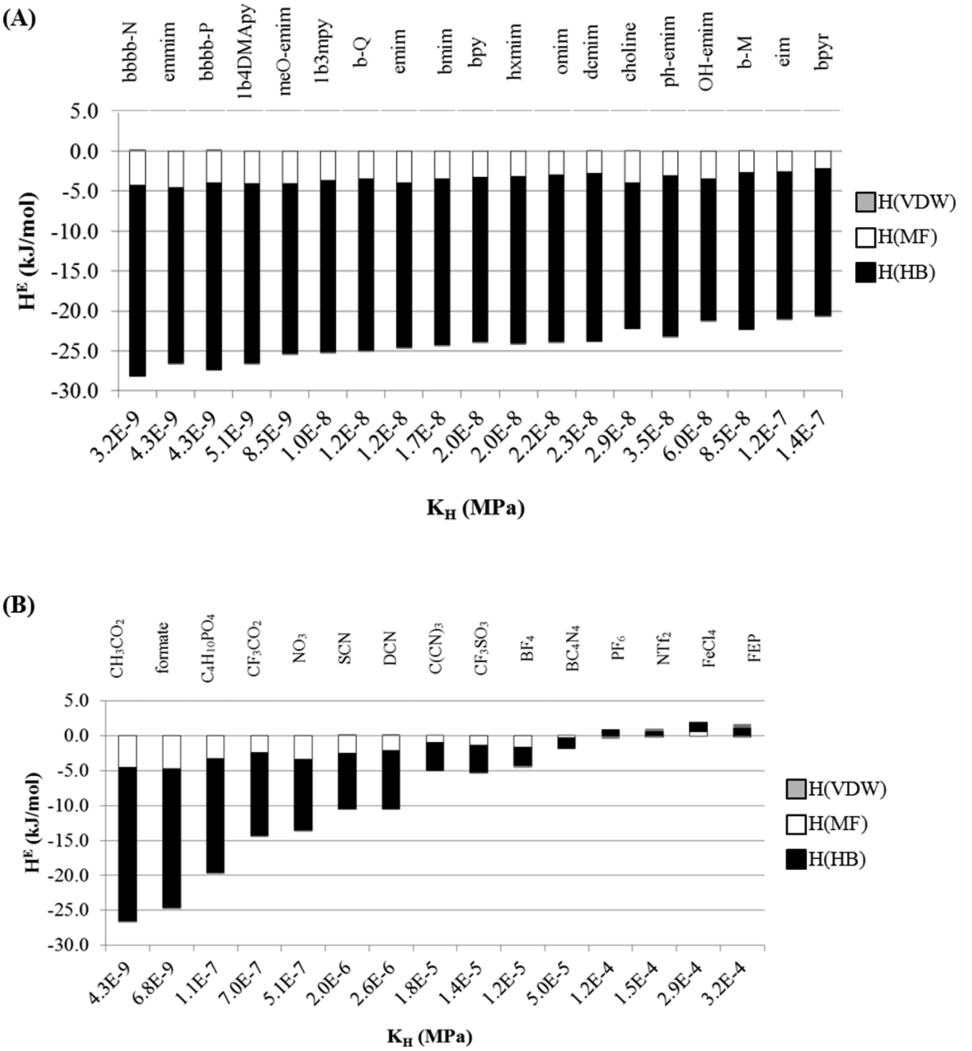

Figure 7. Relationship between the Henry constants (K_H) and the different intermolecular interaction contributions to the excess enthalpy [H(VDW), H(HB), and H(MF)] of phenol−IL systems at T = 298 K computed by COSMO-RS. (A) Effect of the cation considering CH_3CO_2 as the common anion. (B) Effect of the anion considering emmim as the common cation.

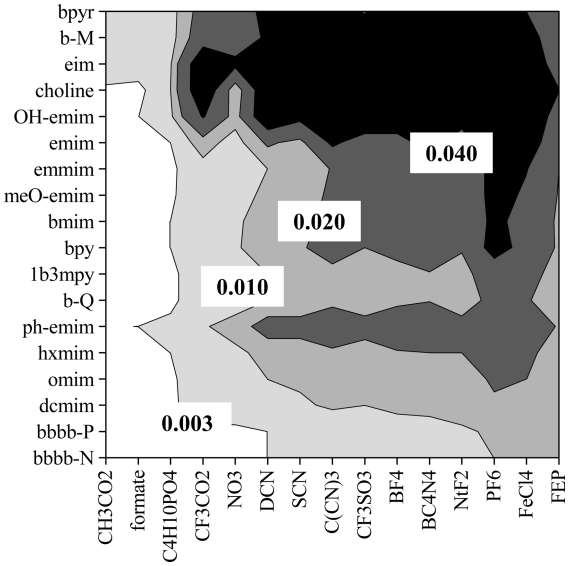

Figure 8. Screening of the Henry constants (MPa) of chloroform in ILs at T = 298 K computed by COSMO-RS.

intermolecular interactions. The selection of cations in the absence of strong HB donor groups, i.e., [emmim$^+$], [bbbb-P$^+$], or [bbbb-N$^+$], also increases the absorption, mainly for the case of anions with intermediate HB acceptor character, such [$CF_3SO_3^-$]. Figure 9 shows the relationship between the Henry constants and the different contributions to the excess enthalpy of the chloroform−ILs mixtures. As for the case of the acetone, the results indicate that the attractive hydrogen-bonding interactions determine the solubility between the solute and the solvent, while the electrostatic interactions play a secondary role, and the van der Waals interactions almost do not contribute to the excess enthalpy of the liquid mixture. However, in the case of the chloroform solute, the attractive hydrogen-bonding interactions which control the solubility are those between the acidic hydrogen atom of chloroform and the basic groups of the ions of the IL solvents. Figure 9A illustrates the higher affinity of the solute for the least acidic cations, as in the case of [emmim$^+$] > [emim$^+$] > [eim$^+$]; the length of the alkyl chain does not cause noticeable change of the hydrogen-bonding attraction as exemplified by the imidazolium series from [emim$^+$] to [dcmim$^+$]; as for the head family, results suggest that imidazolium, ammonium, and phophonium work better than pyridinium-, pyrrolidinium-, or morpholinium-

dx.doi.org/10.1021/jp310499p | J. Phys. Chem. B XXXX, XXX, XXX−XXX

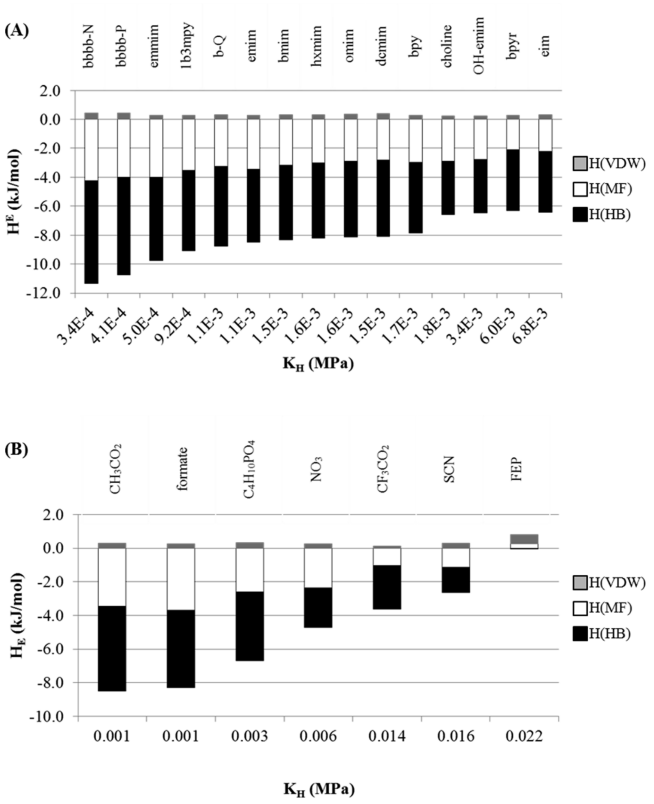

Figure 9. Relationship between the Henry constants (K_H) and the different intermolecular interaction contributions to the excess enthalpy [H(VDW), H(HB), and H(MF)] of chloroform−IL systems at T = 298 K computed by COSMO-RS. (A) Effect of the cation considering CH_3CO_2 as the common anion. (B) Effect of the anion considering emim as the common cation.

based cations. This is most likely because the latter tends to present more acidic character than the former, hence promoting hydrogen bonding between the cation and the anion in detriment of chloroform−anion interactions (see Table 3). As for the effect of the anion, Figure 9B shows the significantly higher affinity of the chloroform for the most basic ions, such as $[CH_3CO_2^-]$ or formate rather than $[FEP^-]$.

3.5. Evaluation of the Overall Trends of VOCs Solubility in ILs. In order to provide a general evaluation of the influence of the structure of ILs on the solubility of VOCs, we have selected a representative sample of 14 organic compounds, including alkanes, alkenes, halogenated, aromatics, esters, and ketones. The COSMO-RS screening was performed for each one of the selected solutes over 135 imidazolium-based ILs, with the aim to provide an overview of the gas solubility behavior of VOCs in ILs. For this purpose, the extreme cases corresponding to the solute−IL systems with the lowest [γ^∞(min)] and the highest [γ^∞(max)] activity coefficient values were identified, and the results are collected in Table 3, A and B, respectively. The minimum activity coefficient, γ^∞(min), is associated to the most favorable IL structure to absorb the VOC solute, whereas the maximum activity coefficient, γ^∞(max), is associated to the worst IL structure to absorb the VOC solute. In order to show more clearly the data reported in the mentioned table (Table 3A,B), the values obtained for the γ^∞(min) and γ^∞(max) for each one of the VOCs solutes in the ILs are illustrated in Figure 10. Moreover, throughout this document the effect that the chemical structure of both VOC

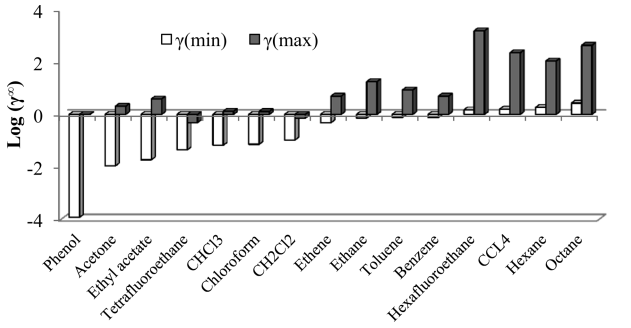

Figure 10. Minimum (γ_{min}) and maximum (γ_{max}) values of activity coefficients at infinite dilution (γ^∞) of VOCs in ILs obtained from COSMO-RS screening at 298 K over 135 imidazolium-based ILs.

and IL has on the solute−solvent interactions which determine the absorption capability has been discussed. For that reason, the energetic contributions to the excess enthalpy of the VOC-IL systems that present γ^∞(min) is collected in Table S23 in the Supporting Information. Figure 11 shows a plot of those

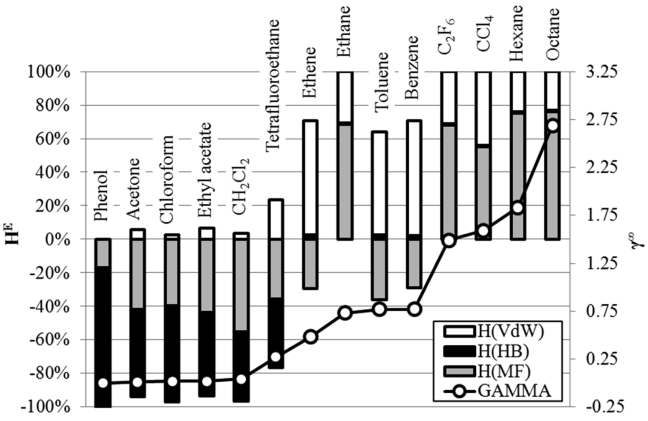

Figure 11. Relationship between the minimum values of activity coefficients at infinite dilution, γ^∞(min), and the percentages of the different intermolecular interaction contributions to the excess enthalpy [H(VDW), H(HB), and H(MF)] for VOCs in ILs reported in Table 3, computed by COSMO-RS at T = 298 K.

different energetic contributions expressed as percentages, in order to visually represent the data more clearly. On the basis of these results, we propose the following classification of VOC compounds respect to their solubilities on ILs, considering the effect of rationally selecting the cationic and anionic species for a potential absorption process:

(i) VOCs with favorable absorption in ILs: solutes containing strong polar functional groups with remarkable HB donor/acceptor character, such as phenol, acetone, ethyl acetate, and chloroform. Considering the noticeably low values of γ^∞(min) < 0.1, these solutes exhibit a strong negative deviation from ideality. These solutes are classified as group 1 in Table 2, and present very low values of Henry's constant (Table 3A) and an overall high solubility in ILs. The gas solubility behavior of this kind of VOCS in ILs is mainly determined by HB interactions (Table 3, Figure 11). Hence, the affinity of the IL solvent for these VOC solutes can be greatly enhanced selecting an adequate anion−cation combination that promote attractive hydrogen bonding between the solute and the IL.

(ii) VOCs with moderate absorption in ILs: solutes containing short alkyl chains or aromatic character (i.e., ethane,

dx.doi.org/10.1021/jp310499p | J. Phys. Chem. B XXXX, XXX, XXX−XXX

ethene, benzene) which exhibit activity coefficients in ILs with a moderate negative deviation from ideality ($0.1 < \gamma^{\infty}(\min) \leq 1$). The solubility behavior of these solute−solvent systems, i.e., VOCs whose absorption can be moderately enhanced by selecting adequate ILs, is generally determined by van der Waals interactions (which are weaker in the mixture than in the pure fluid, providing endothermic contributions) and favorable polar-misfit interactions between the VOC solute and the IL solvent (Table 3A, Figure 11). The most appropriate ILs to enhance the solubility of most of these VOCS are those composed of cations with long alkyl chains and large anions with disperse charge like [FEP$^-$]. It is should be noted that the moderate IL capacity to absorb these VOCs (classified as groups 2 and 3 in Table 2) depends on both the relatively low activity coefficients and the vapor pressure of pure solute compound. This is evident for the tetrafluoethane/ethane/toluene series, which presents increasing $\gamma^{\infty}(\min)$ trend (0.27/0.73/0.77) but a variety of gas solubilities in terms of K_H values (1.6×10^{-1}/6.0/3.3×10^{-3}), due to the different volatility of the solutes.

(iii) VOCs with unfavorable absorption in ILs: aliphatic solutes such as hexane or octane and perhalogenated compounds such as CCl_4 which present high values of $\gamma^{\infty}(\min) > 1$; this indicates a positive deviation from ideality (Table 3A, Figure 11), and hence a higher volatility of the solute in the IL than that of the pure compound. All these solutes exhibit unfavorable solute−solvent interactions, with their solubilities in ILs ranging from very low (VOCs classified as group 4 in Table 2, with high vapor pressure of pure compound) to intermediate (VOCs with high molar weight and relatively low vapor pressure). Figure 11 shows that the unfavorable solubility behavior of these VOCs in ILs is related to the repulsive electrostatic interactions. Moreover, Table 3B and Figure 10 show that the solubility of these solutes in ILs can be strongly diminished by selecting small imidazolium cations and polar anions such as [SCN$^-$] that promote repulsive electrostatic interactions with the nonpolar compounds included in this type of VOCs. These [SCN$^-$]-based ILs can be applied in aliphatic/aromatic separation (i.e., heptane/benzene[53]) or in oil desulfurization processes,[54] including extractive membrane technologies to separate organosulfur compounds from refinery products.[55]

4. CONCLUSIONS

A systematic COSMO-RS analysis of the thermodynamics and energetic interactions of a wide sample of VOC−IL systems was performed. COSMO-RS shows a general predictability of the gas solubility behavior of different solutes in ILs. A clear relationship between the activity coefficient at infinite dilution (γ^{∞}) of solutes in the ILs and the excess enthalpy (H^E) of the equimolar IL−solute mixtures was reported, observing a remarkably negative deviation from Raoult's law for strong exothermic VOC−IL mixtures. A comprehensive gas solubility screening and detailed energetic analysis of three representative polar VOCs (acetone, phenol, and chloroform) in ILs systems indicated that favorable solute−solvent interactions can be conveniently tuned by cation and anion selection, enhancing the gas solubility of these VOCs in ILs. Finally, the COSMO-RS study was extended to a sample of 14 representative VOCs with strong structural differences, with results leading to propose a classification of VOCs respect to their solubilities in ILs. This classification gave an insight into the rational selection of the cationic and anionic species that provided, respectively, the highest negative and positive deviations from the ideality and, consequently, the most favorable and unfavorable properties to absorb VOCs in ILs.

■ ASSOCIATED CONTENT

Supporting Information

Table S1: Experimental and COSMO-RS Henry constants of solutes in ILs at near-ambient temperature and atmospheric pressure using vapor pressures of pure compounds predicted by COSMO-RS and estimated by empirical Antoine equation. Tables S2−S4: Screening of the Henry constants of acetone, phenol, and chloroform in ILs at T = 298 K computed by COSMO-RS. Table S5−S22: Screening of the activity coefficients and excess enthalpy of acetone, benzene, chloroform, ethane, ethane, phenol, H_2S, H_2, and trifluoroethane in ILs at T = 298 K computed with COSMO-RS. Table S23: Activity coefficients, excess enthalpies, and intermolecular interaction contributions of VOCs in ILs at T = 298 K computed by COSMO-RS. This material is available free of charge via the Internet at http://pubs.acs.org.

■ AUTHOR INFORMATION

Corresponding Author

*Tel.: 34 91 4976938. Fax: 34 91 4973516. E-mail: pepe.palomar@uam.es.

Notes

The authors declare no competing financial interest.

■ ACKNOWLEDGMENTS

The authors are grateful to the Ministerio de Economía y Competitividad and Comunidad de Madrid for financial support (projects CTQ2011-26758 and S2009/PPQ-1545, respectively).

■ REFERENCES

(1) Huddleston, J. G.; Willauer, H. D.; Swatloski, R. P.; Visser, A. E.; Rogers, R. D. *Chem. Commun.* **1998**, 1765−1766.
(2) Tokuda, H.; Hayamizu, K.; Ishii, K.; Abu Bin Hasan Susan, M.; Watanabe, M. *J. Phys. Chem. B* **2004**, *108*, 16593−16600.
(3) Tokuda, H.; Hayamizu, K.; Ishii, K.; Abu Bin Hasan, M.; Susan, M. Watanabe. *J. Phys. Chem. B* **2004**, *109*, 6103−6110.
(4) Wasserscheid, P.; Welton, T. *Ionic Liquids in Synthesis*; Wiley-VCH: Weinheim, Germany, 2008.
(5) Huang, J.; Reuther, T. *Aust. J. Chem.* **2009**, *62*, 298−308.
(6) Bara, J. E.; Carlisle, T. K.; Gabriel, C. J.; Camper, D.; Finotello, A.; Gin, I.; Gin, D. L.; Noble, R. D. *Ind. Eng. Chem. Res.* **2009**, *48*, 2739−2751.
(7) Lu, X. Y.; Burrel, G.; Separovic, F.; Zhao, C. *J. Phys. Chem. B* **2012**, *116*, 9160−9170.
(8) Anderson, J. L.; Dixon, J. K.; Brennecke, J. F. *Acc. Chem. Res.* **2007**, *40*, 1208−1216.
(9) Camper, D.; Becker, C.; Koval, C.; Noble, R. *Ind. Eng. Chem. Res.* **2005**, *44*, 1928−1933.
(10) Carlisle, T. K.; Bara, J. E.; Gabriel, C. J.; Noble, R. D.; Gin, D. L. *Ind. Eng. Chem. Res.* **2006**, *45*, 6279−6283.
(11) Condemarin, R. A.; Scovazzo, P. *Chem. Eng. J.* **2009**, *147*, 51−57.
(12) Kilaru, P. K.; Scovazzo, P. *Ind. Eng. Chem. Res.* **2008**, *47*, 910−919.
(13) Kumełan, J.; Perez-Salado Kamps, A.; Tuma, D.; Maurer, G. *J. Chem. Eng. Data* **2006**, *51*, 1802−1807.
(14) Jacquemin, J.; Husson, P.; Majer, V.; Padua, A. H.; Costa-Gomes, M. F. *Green Chem.* **2008**, *10*, 944−950.
(15) Raeissi, S.; Peters, C. J. *Green Chem.* **2009**, *11*, 185−192.

(16) Almantariotis, D.; Gefflaut, T.; Padua, A. A. H.; Coxam, J. Y.; Costa-Gomes, M. F. *J. Phys. Chem. B* **2010**, *114*, 3608−3617.
(17) Jalili, A. H.; Rahmati-Rostami, M.; Ghotb, C.; Hosseini-Jenab, M.; Ahmadi, A. Naser *J. Chem. Eng. Data* **2009**, *54*, 1844−1849.
(18) Costa-Gomes, M. F. *J. Chem. Eng. Data* **2007**, *52*, 472−475.
(19) Jacquemin, J.; Husson, P.; Majer, V.; Costa-Gomes, M. F. *Fluid Phase Equilib.* **2006**, *240*, 87−95.
(20) Jacquemin, J.; Costa-Gomes, M. F.; Husson, P.; Majer, V. *J. Chem. Thermodyn.* **2006**, *38*, 490−502.
(21) Kumełan, J.; Perez-Salado Kamps, A.; Tuma, D.; Maurer, G. *Fluid Phase Equilib.* **2007**, *260*, 3−8.
(22) Kumean, J.; Perez-Salado Kamps, A.; Tuma, D.; Maurer, G. *Ind. Eng. Chem. Res.* **2007**, *46*, 8236−8240.
(23) Kumean, J.; Perez-Salado Kamps, A.; Tuma, D.; Maurer, G. *J. Chem. Eng. Data* **2007**, *52*, 2319−2324.
(24) Anderson, J. L.; Dixon, J. K.; Maginn, E. J.; Brennecke, J. F. *J. Phys. Chem. B* **2006**, *110*, 15059−15062.
(25) Palomar, J.; Gonzalez-Miquel, M.; Bedia, J.; Rodríguez, F.; Rodríguez, J. J. *Sep. Purif. Technol.* **2011**, *82*, 43−52.
(26) Bedia, J.; Palomar, J.; Gonzalez-Miquel, M.; Rodriguez, F.; Rodriguez, J. J. *Sep. Purif. Technol* **2012**, *95*, 188−195.
(27) Camper, D.; Becker, C.; Koval, C.; Noble, R. *Ind. Eng. Chem. Res.* **2006**, *45*, 445−450.
(28) Lee, B. C.; Outcalt, S. L. *J. Chem. Eng. Data* **2006**, *51*, 892−897.
(29) Shiflett, M. B.; Yokozeki, A. *Ind. Eng. Chem. Res.* **2006**, *45*, 6375−6382.
(30) Kumelan, J.; Perez-Salado Kamps, A.; Tuma, D.; Yokozeki, A.; Shiflett, M. B.; Maurer, G. *J. Phys. Chem. B* **2008**, *112*, 3040−3047.
(31) IUPAC Ionic Liquids Database (IL Thermo), www.ilthermo.boulder.nist.gov.
(32) Quijano, G.; Couvert, A.; Amrane, A.; Darracq, G.; Couriol, C.; Le Cloirec, P.; Paquin, L.; Carrié, D. *Chem . Eng. J.* **2011**, *66*, 2707−12.
(33) Bedia, J.; Ruiz, E.; de Riva, J.; Ferro, V. R.; Palomar, J.; Rodriguez, J. J. *AIChE J.* **2012**, DOI: 10.1002/aic.13926.
(34) Klamt, A.; Eckert, F.; Arlt, W. *Annu. Rev. Chem. Biom. Eng.* **2010**, *1*, 101−122.
(35) Diedenhofen, M.; Klamt, A. *Fluid Phase Equilib.* **2010**, *294*, 31−38.
(36) Palomar, J.; Torrecilla, J. S.; Ferro, V. R.; Rodríguez, F. *Ind. Eng. Chem. Res.* **2008**, *47*, 4523−4532.
(37) Palomar, J.; Torrecilla, J. S.; Ferro, V. R.; Rodríguez, F. *Ind. Eng. Chem. Res.* **2009**, *48*, 2257−2265.
(38) Zhang, X.; Liu, Z.; Wang, W. *AIChE J.* **2008**, *54* (10), 2717−2728.
(39) Manan, N. A.; Hardacre, C.; Jacquemin, J.; Rooney, D. W.; Youngs, T. G. *J. Chem. Eng. Data* **2009**, *54*, 2005−2022.
(40) Palomar, J.; Gonzalez-Miquel, M.; Polo, A.; Rodríguez, F. *Ind. Eng. Chem. Res.* **2011**, *50*, 3452−3463.
(41) Gonzalez-Miquel, M.; Palomar, J.; Omar, S.; Rodríguez, F. *Ind. Eng. Chem. Res.* **2011**, *50*, 5739−5748.
(42) Sistla, Y. S.; Khanna, A. *J. Chem. Eng. Data* **2011**, *56*, 4045−4060.
(43) Sumon, K. Z.; Henni, A. *Fluid Phase Equilib.* **2011**, *310* (1−2), 39−55.
(44) Navas, A.; Ortega, J.; Vreekamp, R.; Marrero, E.; Palomar, J. *Ind. Eng. Chem. Res.* **2009**, *48*, 2678−2690.
(45) Oyama, S. T.; Hunter, P. *Control of Volatile Organic Compounds Emissions: Conventional and Emerging Technologies*; Wiley-Interscience: New York, 2000.
(46) Clean Air Act Amendments. National Air Quality and Emissions Trends Report; EPA, USA, 1998.
(47) Directive 2001/81/EC of the European Parlament and of the Council of 23 October 2001 on national emission ceilings for certain atmospheric pollutants.
(48) Building Assessment Survey and Evaluation Study: Volatile Organic Compounds. EPA, USA, 2012. http://www.epa.gov/iaq/base/voc_master_list.html
(49) Frisch, M. J.; Trucks, G. W.; Schlegel, H. B.; Scuseria, G. E.; Robb, M. A.; Cheeseman, J. R.; Montgomery, J. A.; Vreven, T.; Kudin, K. N.; Burant, J. C.; Millam, J.M.; Iyengar, S. S.; Tomasi, J.; Barone, V.; Mennucci, B.; Cossi, M.; Scalmani, G.; Rega, N.; Petersson, G. A.; Nakatsuji, H.; Hada, M.; Ehara, M.; Toyota, K.; Fukuda, R.; Hasegawa, J.; Ishida, M.; Nakajima, T.; Honda, Y.; Kitao, O.; Nakai, H.; Klene, M.; Li, X.; Knox, J. E.; Hratchian, H. P.; Cross, J. B.; Bakken, V.; Adamo, C.; Jaramillo, J.; Gomperts, R.; Stratmann, R. E.; Yazyev, O.; Austin, A. J.; Cammi, R.; Pomelli, C.; Ochterski, J. W.; Ayala, P. Y.; Morokuma, K.; Voth, G. A.; Salvador, P.; Dannenberg, J. J.; Zakrzewski, V. G.; Dapprich, S.; Daniels, A. D.; Strain, M. C.; Farkas, O.; Malick, D. K.; Rabuck, A. D.; Raghavachari, K.; Foresman, J. B.; Ortiz, J. V.; Cui, Q.; Baboul, A. G.; Clifford, S.; Cioslowski, J.; Stefanov, B. B.; Liu, G.; Liashenko, A.; Piskorz, P.; Komaromi, I.; Martin, R. L.; Fox, D. J.; Keith, T.; Al-Laham, M. A.; Peng, C. Y.; Nanayakkara, A.; Challacombe, M.; Gill, P. M.; Johnson, B.; Chen, W.; Wong, M. W.; González, C.; Pople, J. A. *Gaussian03, revision B.05*; Gaussian, Inc.: Wallingford, CT, 2004.
(50) *COSMOtherm C2.1 Release 01.11*; COSMOlogic GmbH & Co. KG: Leverkusen, Germany, 2010; http://www.cosmologic.de.
(51) Eckert, F.; Klamt, A. *AlChE J.* **2002**, *48* (2), 369−382.
(52) Klamt, A.; Eckert, F. *Fluid Phase Equilib.* **2000**, *172*, 43−72.
(53) Domańska, U.; Królikowska, M. *J. Chem. Eng. Data* **2011**, *56*, 124−129.
(54) Kedra-Królik, K.; Fabrice, M.; Jaubert, J. N. *Ind. Eng. Chem. Res.* **2011**, *50*, 2296−2306.
(55) Petra, C.; Katalin, B. B. Application of Ionic Liquids in Membrane Separation Processes, Ionic Liquids: Applications and Perspectives; 2011. ISBN: 978-953-307-248-7. Available from: http://www.intechopen.com/books/ionic-liquids-applications-and-perspectives/application-of-ionic-liquids-in-membrane-separation-processes.